Calibration and Validation Concept for the Airborne PRISM Experiment (APEX)

D. Schläpfer, M. Schaepman, S. Bojinski, and A. Börner

Remote Sensing Laboratories (RSL),

Department of Geography, University of Zurich, CH-8057 Zurich, Switzerland

Phone: +41 1 635 52 50, Fax: +41 1 635 68 46, E-mail: dschlapf@geo.unizh.ch

Abstract

The development of the Airborne PRISM Experiment (APEX) is supported by the European Space Agency (ESA) in view of an appropriate data simulator for future spaceborne hyperspectral instruments of the Agency. The terminology and conceptual design of the calibration and validation steps required for the APEX system are defined in this paper. The calibration concept for the APEX instrument is based on a standardized laboratory procedure in which spectral response, geometric response, as well as radiometric gain and offset values are determined. Additionally, in-flight calibration using sensor-internal means and vicarious calibration approaches will improve the reliability of the calibrated image data. All calibration-related parameters as well as the image data are kept and administered by the APEX Processing and Archiving Facility (PAF). A processing chain is defined which allows an efficient preparation of all the calibration parameters and fully reproducible processing of the acquired data from raw format to calibrated radiances. The validation concept for the imagery and its processing is based on sensor simulation, standard quality control procedures, and in-flight validation campaigns. The combination of all these efforts results in a consistent characterization of the APEX instrument performance and a reliable quality definition of the final image data products.

accepted as technical note in the *Canadian Journal of Remote Sensing*, February 2000.

Résumé

Le développement du projet “Airborne PRISM Experiment (APEX)” est menée par l’Agence Spatiale Européenne (ESA) dans le cadre de simulations de ses futurs instruments satellitaire hyperspectrals. Cette article développe la terminologie ainsi que le modèle conceptuel des étapes de calibration et de validation nécessaires au système APEX. Le processus de calibration de l’appareil APEX suit une procédure de laboratoire standardisée où les réponses spectrales et géométriques ainsi que le gain et les biais radiométriques sont détérminés. En outre, la calibration en vol , s’appuyant sur des procédés à base de capteurs internes et de calibration vicariaux, permettent d’améliorer la qualité de l’image obtenue. L’ensemble des paramètres définis et l’image son administrés par une gestionnaire de données dédié dans la “Apex Processing and Archiving Facility (PAF)”. Une chaîne de traitement est définie afin de garantir une préparation efficace des paramètres de calibration et de permettre une reproduction exacte du traitement, des données brutes jusqu’au radiances calibrées. Le modèle de validation s’applique non seulement à l’image mais aussi au traitement lui-même. Il se base sur la simulation de l’instrument, des processus standards de contrôle qualité, et de missions de validation en vol. La combinaison de tous ces points offre à l’appareil APEX des performances garantissant la qualité des images fournies.

Glossary

c	Spectral band index
DC_i	Dark current per detector element
$DN_i(L)$	Digital signal at detector after A/D conversion (in digital numbers)
$DN_{max,\,i}$	Maximal digital output of a detector element during radiometric calibration
$DN_{NER,\,i}$	Noise equivalent digital signal (at NER level) per detector element
$FWHM_c$	Spectral resolution of a spectral band at ‘full width at half maximum’
$FWHM_x$	Spatial PSF resolution across track at ‘full width at half maximum’
$FWHM_y$	Spetial PSF resolution along track at ‘full width at half maximum’

g_i	Gain per detector element
i, j	Detector element indices
L	Radiance
$L_{im,i}$	Image radiance value as stored in the calibrated image data file (scaled)
$\overline{L_{im,j}}$	Interpolated image radiance value for bad pixel replacement
$L_{bp,i}$	Interpolated image radiance for a bad pixel
L_{NER}	Noise equivalent radiance
L_{dark}	Apparent radiance at closed shutter
L_{max}	Maximal radiance during calibration
λ_c	Central wavelength for spectral band
PSF_x / PSF_y	Spatial point spread function of the image pixels
$\lambda_{min} / \lambda_{max}$	Wavelength range for spectral calibration
r_i	Responsivity of a detector element
s	Scale factor to store calibrated radiance values in 2-byte integer words
SNR_i	Signal to noise ratio per detector element
SNR_c	Signal to noise ratio per spectral band
x	Across track image dimension
x_{min} / x_{max}	Range of slit movement during geometric across track calibration
y	Along track image dimension
y_{min} / y_{max}	Range of slit movement during geometric along track calibration

Introduction

Starting in 1997, the development of the Airborne PRISM Experiment (APEX; Itten et al., 1997) is supported by the European Space Agency (ESA). The APEX instrument is intended to be an airborne hyperspectral data simulator for the future Land Mission LSPIM (Labandibar et al., 1999; Rast and Silvestrin, 1999). APEX will scan the earth's surface using a "pushbroom" imager with up to 300 spectral bands. The wavelength range between 400 and 2500 nm is covered by two detector arrays with approximately 1000 pixels per scan line and at a spectral sampling interval of 5 to 10 nm. The ground pixel

size ranges from 2 to 5 m at a flight altitude of 4 to 10 km. The sensor is expected to be operational by the year 2002. Simultaneously to the hardware construction of the instrument, the Processing and Archiving Facility (PAF) for APEX is set up and implemented.

The calibration concept for APEX has to be defined prior to the development of the hardware and the implementation of the software since the different parts have to match each other. We first define the number and type of measurements to be taken for sensor calibration during its operational phase. An unambiguous terminology helps to structure all data acquisition processes.

The subsequent transformation of the image data to physical units has to be handled efficiently by the PAF. The corresponding concept for the image calibration process defines the standard processing steps and the process outputs up to the system calibrated image data level.

No calibration can be done without considering its validation. Thus, the accuracy of the results will be controlled using dedicated vicarious calibration campaigns and data simulations. Further quality control of the image data itself is required for a highly automated supervision of the system performance (cf. Teillet et al., 1997).

Calibration Strategy

The calibration strategy for the APEX system includes a wide variety of measurements during regular data acquisition and during dedicated calibration campaigns. The time schedule of the individual data takes and the type of measurements to be taken are defined hereafter.

An overall radiometric accuracy of better than 2% at any time compared to an established laboratory standard has been defined as a mandatory requirement for the APEX system. This accuracy can be met using a three level strategy including laboratory, in-flight, and vicarious calibration experiments. The goal of these calibration efforts is the conversion of the raw digital numbers as measured by the imaging instrument to physical units with an absolute accuracy below ± 4% (cf. Chrien et al., 1990; Thome et al., 1998), including the inherent traceability errors of laboratory standards (Fox, 1999).

Data Acquisition Terminology

The terminology for the data acquisition and the scheduling of the calibration tasks is depicted in Figure 1. It includes the strategic positions of the three calibration levels including vicarious calibration campaigns, laboratory measurements, and the on-board calibration means.

A *flight cycle* is usually represented by a flight season in which various campaigns are flown, given by different time-frames and locations. If the sensor is technically revised during a flight cycle, a new laboratory and vicarious calibration campaign is required. This process is repeated at the end of a flight cycle just before the sensor is dismantled or taken into a major revision. A *sensor revision* is treated as a logical unit because the instrument characteristics may alter in the course of such a construction period.

An *APEX campaign* is synonymous to a *flight cluster* and is defined by an organizational time-frame from the operator's point of view. Each flight is then represented by the on-board *flight storage capacity,* amounting approximately 200 GB. It is subdivided into *recording units* (e.g. swappable hard disks) according to the total capacity of one storage medium.

A *research campaign* can either be a part of one flight or consists of several flights within the same geographic area. It is defined by a specific Principle Investigator (PI). The research campaigns can differ from the APEX campaigns, which in contrast are defined by organizational and technical presuppostions such as airplane availability, sensor condition, flight storage capacity, processing capacity, or staff availability.

A number of *sections* may be flown in the course of one research campaign at different locations or days (for technical reasons, each section is also a sub-part of the recording units). The on-board calibration data are taken before and after each image section. If a flight pattern is flown over a specific geographic area, the section is subdivided into *runs*, given by single, continuously registered image stripes. A run usually will consist of up to 15'000 lines, corresponding to a data volume of up to 9 GB. This data volume is too large to be handled efficiently. Therefore, it has been decided to cut the runs into *scenes* of up to 1500 image lines each for further processing within the PAF.

The levels of data acquisition as defined above are also used for data storage and retrieval in the APEX database system. The processing steps of the PAF are usually related to the scene level, while most of the attribute data are stored in higher levels (e.g. per run, section, or sensor revision).

Laboratory Calibration

Based on the flexibility of the APEX instrument to be integrated into an aircraft within less than three hours, frequent laboratory calibration cycles are foreseen to monitor the stability of the instrument. The laboratory calibration setup of APEX includes radiometric, spectral, and geometric calibration (cf. Bruegge et al., 1998; Schaepman, 1998). The measurements themselves will be taken as single runs using the instrument in calibration mode. The proposed laboratory calibration measurements will result in data cubes as depicted in Figure 2.

Radiometric Calibration

The radiometric calibration is performed using an integrating sphere which is traceable to a national standard, such as maintained by NIST (National Institute for Standards and Technology, USA) or NPL (National Physics Laboratories, GB). Best results will be achieved if a primary standard of one of these institutions is used for (cross-)calibration of the sphere (Fox, 1999).

The laboratory sphere is also intended to be used to intercalibrate the sphere that is built into the instrument itself in order to establish it as a secondary standard. The traceability of the instrument sphere is specified to be within ≤ 2% of the laboratory sphere. Its traceability has to be updated during each laboratory campaign to ensure this degree of accuracy.

For the radiometric calibration, the luminosity of the sphere has to be increased gradually during data acquisition. First, the response function is determined using increasing intervals up to the saturating level L_{max} (see Figure 2). Secondly, the level of the noise equivalent radiance L_{NER} has to be measured as standard deviation σ of the signal at closed shutter, given by $DN(L_{NER}) = \sigma(DN(L_{dark}))$. The amount of L_{NER} itself can then be derived using the previously measured radiometric response characteristics.

Spectral Calibration

The spectral calibration aims at a center wavelength accuracy of 0.2 nm and at 2% relative accuracy of the spectral sampling width (cf. Green, 1998). A monochromator coupled with a collimator is used as source to take the measurements at a spectral resolution according to the required accuracy. This results in more than 10’000 lines of calibration measurements to achieve the wavelength dependent spectral response functions of each detector pixel individually.

Geometric Calibration

Finally, the geometric calibration of the instrument resolves the spatial Point Spread Function (PSF) distortions across track and along track. A slit illuminated by a spectrally homogeneous collimated source can be moved along and across the sensor field of view at spatial intervals of 0.1 times the detector pixel size. The across track measurement effort can be rationalized using a moving aperture of illuminated parallel slits (Figure 2, lower right). This procedure will result in spatial response functions PSF_x across track and PSF_y along track for the steady intrument.

Note that the spatial PSF is not identical to the system PSF. The latter decribes the transfer of one image line through the optics on to the detector arrays which register the spectral and the spatial dimensions simultaneously. It is affected by “smile” effects (spatially dependent misregistrations in spectral direction) and “frown” effects, which affect the spatial co-registration across track of all spectral bands (Fisher et al., 1998). Both effects are kept minimal by optimizing the APEX optical design for low aberrations. The system PSF function can only be inferred from the combination of the geometric and the spectral calibration results.

Stability Monitoring

The laboratory calibration includes also the measurement of temperature dependencies, statistical linearity of the radiometric response, and various other influences on the signal (e.g. polarization, straylight, out-of-band noise). The respective measurements are analyzed and the results are stored in a separate calibration report.

On-board Calibration

The instrument performance needs special attention as long as the instrument resides on its carrier, since pushbroom scanners can not scan a reference source for each detector element during data acquisition. For optimal in-flight stability, the instrument including its on-board calibration means shall be operated in a closed housing with constant pressure and temperature.

Before an image section is acquired, an internal mirror depoints the optical path into the on-board integrating sphere whose pre-defined radiance levels are then registered. Afterwards, a fixed number of dark signal lines is acquired at closed shutter. After mechanically shifting the internal mirror out of the optical path, the normal scene radiance values are acquired. A number of pixels on each side of the

detector array are permanently obscured, monitoring the dark current during data acquisition. Furthermore, housekeeping information is recorded which includes temperature and pressure measurements within the sealed sensor housing. Before the recording devices are switched off, the dark signal and the integrating sphere are scanned a second time. The combination of all acquired on-board calibration data allows for a reconstruction of possible instrument performance drift during data acquisition. A model of an acquired image section is depicted in Figure 3.

Vicarious Calibration

After each sensor revision, vicarious calibration experiments will support the evaluation of the expected instrument performance during its operation on the aircraft. An estimate of the instrument characteristics is obtained for operation in an off-laboratory environment.

A well known calibration test site is overflown while simultaneous in-field spectroradiometric measurements are taken (Strobl et al., 1997). The instrumentation includes field spectroradiometers, the RSL Field Goniometer System (FIGOS; Sandmeier and Itten, 1999), a mobile Sun Photometer (Ehsani and Reagan, 1992), and standard radiosonde measurements. All these data are combined for a most adequate modelling of the ground reflectance measurements to at-sensor radiances using the MODTRAN radiative transfer code (Berk et al., 1989).

The results from vicarious calibration campaigns are mainly used for validation of the laboratory and on-board calibration results. If significant discrepancies are found, additional re-calibration efforts in laboratory are necessary. Furthermore, the vicarious calibration campaigns are used to validate the performance and accuracy of the data processing chain.

Raw Data Processing and Calibration

The processing concept up to at-sensor radiance calibrated data is based directly on the calibration strategy. It includes the data download procedure and the data preparation, denominated as “level 0”, as well as the level 1 image calibration processing steps. In level 0, consistent data file formats are created and the raw data are archived. The radiometry remains unchanged throughout this part of the processing chain. The level 1 processor transforms the prepared raw data values to the required SI units (système

internationale) using the abovementioned results from the sensor calibration efforts. Figure 4 gives a detailed overview on the dataflow as described hereafter.

Starting directly after downloading, all file, scene, and processor attribute data will be administered by the PAF database system. The system is designed in such a way that it allows full control of the data flow and repeatability for every process. Thus, the input parameters for each process have to be logged in the database system along with the raw data and their attributes. This archiving concept allows complete tracking and repeatability of any once performed process.

Image Download and Segregation

The first major step to be performed in the PAF prior to a consistent data processing is the downloading and segregation routine, where the data are archived and converted to appropriate data formats. The APEX sensor data acquired during any data take are initially stored on high capacity disks in sequential order (BIP, Band Interleaved by Pixel). The download itself will be done by connecting the media directly to the PAF computing hardware. During the reading and segregation process, the individual sections (stored on the primary recording units) are split into two entities: on-board calibration data and scenes. The first *n* scenes will have 1500 scanlines each, and the last scene will complete a run. A scene is not subdivided further throughout the processor. All co-registered spectral bands of one scene are finally represented by a data concept called ‘data cube’ or ‘cube’ (compare Figure 3).

After the segregation, the following information will be available in distinct data entities (see Figure 4):

- *Raw image cube*: max. 16 bit digital numbers of the sensor measurements in original BIP representation,
- *Image header*: header information related specifically to the cube, containing dimensions and basic attribute data (e.g. date, sensor, band interleave, description); the image header data are stored in the PAF database for each scene,
- *Pre/post-section calibration*: data taken by the sensor right before and after the section acquisition process (part of the on-board calibration data),
- *Dark current*: measurements on the obscured part of the detector (up to 50 pixels on each side of the detector), and
- *Housekeeping*: synchronization and timing information, temperature values of the detectors,

pressure in the sealed housing, and other status report numbers per scanline.

The position and attitude data will be processed in a separate data stream. They have to be prepared in a dedicated module and are concatenated to one file per scene, containing all positional and angular data synchronized per scanline.

General sensor attribute data such as field of view, optical and electronical characteristics are initially known from the manufacturer and are not subject to change during normal instrument operation. They are stored within the database in separate tables which are updated whenever the sensor or the detector is upgraded or changed in its specifications.

Raw Data Validation and Preparation

After downloading and segregation, two data products are generated automatically for validation purposes:

- A consistency report describes the raw image data with respect to missing data elements and possible recording failures, and
- A quicklook image is created for the visual assessment of the acquired scene. The quicklook will be available to the end users immediately upon data download.

Additionally, standardized calibration files will be created from the sensor calibration measurements which results in spectral, geometric, and radiometric response functions for each detector element (see Figure 4 for an overview of all calibration files).

The spectral and the geometric response functions describe the overall system PSF as measured in the laboratory. They can be transformed to three descriptive calibration files using fitting techniques adapted to the anticipated shape of the response function: The first file contains the central wavelength λ_c and the spectral width ("Full Width at Half Maximum"; $FWHM_c$) per band c. Two other files contain parameters for the across track (PSF_x) and the along track (PSF_y) spatial response. The parametrized spatial PSF is given for the anticipated 1000 spatial pixels across track and stored as relative center positions Δx and Δy together with the widths $FWHM_x$ and $FWHM_y$, respectively.

The radiometric calibration files originate from laboratory or in-flight measurements. The laboratory data is used to derive effective response curves $DN_i(L)$. They are parametrized assuming a linear behavior to obtain calibration gain g_i and dark current offset DC_i values per detector element i at

the position (x, c) on the detector:

$$DN_i(L) = DC_i + g_i L \text{, with} \quad (1)$$

$$g_i = \frac{\Delta DN_i(L)}{\Delta L} \quad \text{and} \quad DC_i = DN_i(L = 0). \quad (2)$$

The deviations from linearity are given by the 'goodness of fit' of this linear approximation to the response.

Furthermore, the amount and distribution of bad pixels on the detector is derived from the radiometric response files (Kieffer, 1996). The responsivity r_i of the detector pixels is derived from the calibration measurement as:

$$r_i = \frac{SNR_i}{SNR_c} = \frac{DN_{max,i} - DN_{NER,i}}{DN_{NER,i}} \cdot \frac{1}{SNR_c}, \quad (3)$$

where $DN_{max,i}$ are the measurements at maximal radiance and $DN_{NER,i}$ at Noise Equivalent Radiance level. SNR_c is a predefined minimal signal to noise ratio per band which defines a full responsivity. The responsivity is scaled in such a manner that pixels with values below zero are considered completely malfunctioning whereas values larger than one denote 'good' pixels.

The two measured calibration levels of the on-board calibration are transformed directly to additional gain and offset values per detector element. This second information on radiometric calibration will be mainly used for validation purposes.

Level 1 Data Calibration Process

All data calibration steps are performed in the level 1 processing chain as depicted in Figure 4. The main task is the conversion of the scene from digital numbers to radiance values [W/(m^2 sr nm)] by applying the corrections for spectral, spatial and radiometric distortions (as described above). The position and attitude data are calibrated to absolute angles and coordinates of the airplane on a separate processing path.

Radiometric Calibration

The raw digital numbers DN_i are transformed to image radiance values $L_{im,i}$ by inversion of the Equations (1) and (2) (Guenther et al., 1998):

$$L_{im,\,i} = \left((DN_i - DC_i)\frac{1}{g_i} \right) \cdot s\,, \qquad (4)$$

The scaling factor s is introduced in order to scale the whole dynamic range of the at-sensor radiance into a 2 byte integer word. Both constants DC_i and g_i are provided per detector pixel, resulting in $1000 \times 300 \times 2$ radiometric calibration constants for the entire array. Non-linear gain responses are not considered in the processor since the sensor is expected to behave linearly for the expected radiance range.

Bad Pixel Replacement

The bad pixel requirement for APEX assumes no bad pixels occurrence in the image data. Anyhow, bad pixels will affect the image quality, since approximately 0.5 – 2% of all detector elements (i.e. 1500 - 6000 elements) may be malfunctioning. The replacement process is based on the bad pixel map which was created during data preparation. It lists the responsivity r_i from Eq. (3) of all detector pixels i and gives information on the nearest neighbor responsive pixels j.

An enhancement of the original data value has to be applied to pixels with low responsivity. (Bi)-linear interpolation is preferred for that process. The interpolation is done within one detector frame (corresponding to one image line) in spectral and spatial direction using the nearest neighbor responsive pixels (Kieffer, 1996). The resulting interpolated image radiance $\overline{L_{im,\,j}}$ is evaluated at the pixel position i and combined with the original value following Equation (5) to obtain the bad pixel corrected image radiance $L_{bp,\,i}$:

$$L_{bp,\,i} = r_i L_{im,\,i} + (1 - r_i) \cdot [\overline{L_{im,\,j}}]_i\,. \qquad (5)$$

If spectral interpolation is applied, such a replacement should be repeated after atmospheric correction to avoid the effects induced by sharp atmospheric absorption features.

However, it is merely possible to meet the specifications in radiometric calibration accuracy for such interpolated data values. As a consequence, the bad pixel maps has to be provided to the end users to allow the exclusion of bad pixels during higher level processing.

Spatial Point Spread Function Correction

The spatial PSF can be described as a convolution function and influences the image quality significantly. If frown and smile effects are minimal according to the APEX specifications (lower than 0.1 pixels), the spatial blurring induced by the PSF can be corrected independently of the spectral domain. The effect can be corrected with filter techniques using the laboratory calibration files together with

sensor movement models (Starck et al., 1998; Schläpfer et al., 1999). The result is an improvement of the spatial resolution – at the cost of an increased noise level.

Such a process is considered as an optional calibration step and will not be applied to the data in the standard preprocessing chain. Anyhow, only a simple deconvolution algorithm can be applied due to the large amount of data to be processed for each scene – otherwise the processing time would exceed the PAF capabilities by far. Detailed information about deconvolution and its associated performance issues can be found in Janssen (1997).

Data Simulation and Quality Control

In order to validate the calibration processor output, methods to model the data of APEX based on the given system specifications are required. We plan to use existing datasets and synthetic data simultaneously. The quality control procedures rely on these data sets for validation of the processor outputs.

Data Simulation

The optimization of the instrument (or parts of it) in a laboratory is very expensive and requires at least a complete bread-board model. Thus, we combine knowledge about the sensor, the object, its environment and the processing software in one computer model. This approach is best suited for calibration purposes in order to test the performance of the processor using modelled input data. The simulation tool SENSOR (Software ENvironment for the Simulation of Optical Remote sensing systems) (Börner et al., 1999) is used for the following tasks:

- Substantiation of the APEX specifications by validating system parameters,
- Optimization of sensor parameters and observation conditions for specific applications,
- Adaptation and evaluation of the processing algorithms within the APEX PAF.

SENSOR consists of two main parts. The first one describes the sensor environment, the second refers to one the remote sensing system itself. The environment model includes the observed object (e.g. the physical surface), the source of the radiation (e.g. sun), and the atmosphere. Using the knowledge of the sensor design and a flight path, the geometric relations between object and sensor are described using a ray-tracing algorithm. Furthermore, the influence of the atmosphere is considered using pre-

calculated MODTRAN lookup-tables to determine the at-sensor radiance for a representative set of atmospheric parameters. The second part simulates the optics and the electronics of the sensor itself. Pre-calculated lookup-tables are used to model effects like distortion, shading, attenuation, etc. The electronic part is described by modules which deal with the most important noise sources (cf. Gumbel, 1996), the analog signal processing chain, and the digitalization of the signal to APEX-equivalent digital numbers.

Another approach of simulating APEX data is the use of existing imaging spectrometry cubes. Data from HyMap (Cocks et al., 1998), AVIRIS (Vane and Goetz, 1988), or other sensors are used to create realistic image cubes as shown in Figure 3. Spectral and spatial interpolation and artificial addition of the on-board calibration data lead to the expected data dimensions (Schläpfer et al, 1999).

An overview of the APEX simulation concept is shown in Figure 5. The two simulation methods can be coupled by applying an atmospheric correction to the real hyperspectral data, converting the reflectance values to APEX wavelength characteristics, and transforming the results to at-sensor radiances using SENSOR. On the other hand, well known reference reflectance spectra are used as inputs for quantitative analyses of the sensor performance. Their direct conversion to at-sensor radiance using the MODTRAN code is compared to the SENSOR results for quantitative error analysis. This approach is required for the validation of the calibration processor, while the quasi-real data are mainly used for the development of imaging spectroscopy applications.

Data Quality Control

The quality of both hardware and software has to be monitored throughout the operational phase of any remote sensing system (Teillet et al., 1997). The presented concept for APEX includes raw data analysis, calibrated data control, and validation experiments and is depicted in Figure 6.

Raw Data

The hardware quality will be controlled based on the raw data acquired in-flight and during laboratory calibration campaigns. Using the auxiliary files, the following parameters are monitored:

- Noise Equivalent Radiance (NER) and Signal to Noise Ratio (SNR),
- Frown and smile effects on the detector,
- Occurrence of bad pixels,

- Missing lines and unsuccessful data takes,
- Temperature and pressure stability within the instrument housing, and
- Dark current drift during data acquisition.

Calibrated Data

The quality control inherently verifies the processing software as soon as data from a level higher than zero are investigated. A number of image based measures will be applied to the level 1D data in order to test the quality of the distributed calibrated images. The related standard control procedures are:

- Creation and evaluation of cross correlation matrices per detector,
- Automatic search for physically improbable artefacts,
- Histogram comparison between various scenes, and
- Image based SNR estimation.

The latter will be made based on the statistics within most homogeneous areas in an image in comparison to the average signal (Schläpfer, 1998b).

Validation Campaigns

Finally, the APEX processor will be tested using data from vicarious calibration or dedicated validation campaigns. The measured in-field reflectance of selected targets is first compared to the outputs of the complete level 2 processing chain (Schläpfer et al., 1998a). This level includes the correction of at sensor radiance values to the ortho-rectified ground reflectance distribution by considering atmospheric and geometric effects. Secondly, the field measurements are modeled to at-sensor radiances using MODTRAN and can be compared to the level 1D data directly at this level. The SENSOR module is then used to convert the radiance data to digital numbers which are equivalent to APEX raw image data. The results from validation campaigns can thus be compared directly to image data as acquired by the sensor.

Conclusions

A concept has been presented for the whole calibration and validation process of APEX. It includes the tasks and definitions related to calibration from the measurement strategy to the processing chain and the quality control procedures.

The principle of the various calibration measurements and their processing has been discussed in detail. It is yet to be decided which hardware to employ for the calibration. Although the hardware type may influence the resolution and type of measurements to be taken in laboratory, the described concept can persist for sensor calibration due to its broad validity.

The treatment of the image data in the Processing and Archiving Facility is defined in order to allow efficient and reproducible handling. The dataflow from data acquisition to level 1D calibration is defined in detail. The level 1 process includes procedures for radiometric data calibration and bad pixel replacement with optional PSF corrections. The processor has now to be implemented and tested on simulated data cubes such that it will be available as soon as the construction of APEX will be finished.

Additionally, the determination of the APEX system performance during its operation has been described. Figures of merit and uncertainty measures will be provided for the calibration stability and accuracy, the performance of the sensor, the reliability of the PAF, and the quality of delivered data.

The presented calibration and validation concept will also be pursued during the operational phase, controlling possible upgrades or degradations of the instrument. The APEX team members commit themselves to as much transparency about the system performance as possible. Based on this policy we anticipate to form a broad APEX user community, consisting of research groups focussing on imaging spectroscopy.

Acknowledgements

This work has been carried out under the contract-no. ESA 13115/98/NL/VJ of the European Space Agency. The authors greatly acknowledge the input from the APEX Science Consultancy Group. We also thank the reviewers for their valuable comments.

References

Berk A., Bernsten L.S., and Robertson D.C., 1989: *MODTRAN: A Moderate Resolution Model for LOWTRAN7.* Air Force Geophysics Laboratory, GL-TR-89-0122, Hanscom AFB, MA, pp. 38.

Börner A., Schaepman M., Schläpfer D., Wiest L., Reulke R., 1999: Simulation of Hyperspectral APEX Data: The SENSOR Approach. *Proc. SPIE*, **3753**:235-246.

Bruegge C.J., Duval V.G., Chrien N.L., Korechoff R.P., Gaitley B.J., and Hochberg E.B., 1998: MISR Prelaunch Instrument Calibration and Characterization Results. *IEEE Trans. on Geosc. and R. S.*, **36(4)**:1186-1198.

Chrien T.G., Green R.O., and Eastwood M.L., 1990: Accuracy of the Spectral and Radiometric Laboratory Calibration of the Airborne Visible/Infrared Imaging Spectrometer (AVIRIS). *Proc. SPIE*, **1298**:37-49.

Cocks T., Jenssen R., Stewart I., Wilson I., and Shields T., 1998: The HyMap™ Airborne Hyperspectral Sensor: The System, Calibration and Performance. *Proc. 1st EARSeL Workshop on Im. Spec.*, EARSeL/RSL, Zürich, pp. 37-42.

Ehsani A.R. and Reagan J.A., 1992: A Microprocessor Based Auto Sun-Tracking Multi-Channel Solar Radiometer System. Digest of IGARSS'92, Houston, TX, pp. 3.

Fisher J., Baumback M., Bowles J., Grossmann J., and Anoniades J., 1998: Comparison of Low-Cost Hyperspectral Sensors. *Proc. SPIE*, **3438**:23-30.

Fox N.P., 1999: Improving the Accuracy and Traceability of Radiometric Measurements to SI for Remote Sensing Instrumentation. *Proc. 4th Int. Airb. R. S. Conf. and Exh.*, ERIM, Ottawa (CA), **I**:304-311.

Green R.O., 1998: Spectral calibration requirement for Earth-looking imaging spectrometers in the solar-reflected spectrum. *Appl. Optics*, **37(4)**:683-690.

Guenther B., Godden D.G., Xiong X., Knight E.J., Qiu S.-Y., Mongomery H., Hopkins M.M., Khayat M.G., and Hao Z., 1998: Prelaunch Algorithm and Data Format for the Level 1 Calibration Products for the EOS-AM1 Moderate Resolution Imaging Spectroradiometer (MODIS). *IEEE Trans. on Geosc. and R. S.*, **36(4)**:1142-1151.

Gumbel H., 1996: System Considerations for Hyper/Ultra Spectroradiometric Sensors. *Proc. SPIE*, **2821**:138-170.

Itten K.I., Schaepman M., De Vos L., Hermans L., Schlaepfer H., and Droz F., 1997: APEX-Airborne Prism Experiment: A New Concept for an Airborne Imaging Spectrometer. *Proc. 3rd Int. Airb. R. S. Conf. and Exh.*, ERIM, Copenhagen (DK), **I**:181-188.

Janssen P.A. (Ed.), 1997: *Deconvolution of Images and Spectra.* Academic Press, San Diego, pp. 514.

Kieffer H.H., 1996: Detection and Correction of Bad Pixels in Hyperspectral Sensors. *Proc. SPIE*, **2821**:93-108.

Labandibar J.-Y., Jubineau F., Silvestrin P., and Del Bello U., 1999: The ESA Earth Explorer Land Surface Processes and Interactions Mission. *Proc. SPIE*, **3753**:12-23.

Rast M., and Silvestrin P., 1999: *Land Surface Processes and Interactions Mission.* ESA, Reports for Mission Selection, SP-1233(2), pp. 211.

Sandmeier S.R. and Itten K.I., 1999: A Field Goniometer System (FIGOS) for Acquisition of Hyperspectral BRDF Data. *IEEE Trans. on Geosc. and R. S.*, **37(2)**:978-986.

Schaepman M.E., 1998: *Calibration of a Field Spectroradiometer*. Remote Sensing Series, RSL, Zürich, Vol. 31, pp. 145.

Schläpfer D., Schaepman M., and Itten K.I., 1998a: Level II Pre-Processing Concept for the Airborne PRISM Experiment (APEX). *Proc. 1st EARSeL Workshop on Im. Spec.*, EARSeL/RSL, Zürich, pp. 89-96.

Schläpfer D., 1998b: *Differential Absorption Methodology for Imaging Spectroscopy of Atmospheric Water Vapor*. Remote Sensing Series, RSL, Zürich, Vol. 32, pp. 131.

Schläpfer D., Börner A., and Schaepman M., 1999: The Potential of Spectral Resampling Techniques for the Simulation of APEX Imagery based on AVIRIS Data. Summaries of the Eighth JPL Airborne Earth Science Workshop, JPL, Pasadena (CA), pp. 7 (in press).

Starck J.-L., Murtagh F., and Bijaoui A., 1998: *Image Processing and Data Analysis.* Cambridge University Press, pp. 286.

Strobl P., Müller A., Schläpfer D., and Schaepman M., 1997: Laboratory Calibration and In-flight Validation of the Digital Airborne Imaging Spectrometer DAIS 7915. *Proc. SPIE,* **3071**:225-236.

Teillet P.M., Horler D.N.H., and O'Neill N.T., 1997: Calibration, Validation, and Quality Assurance in Remote Sensing: A New Paradigm. *Can. J. of R. S.*, **23(4)**:401-414.

Thome K., Arai K., Hook S., Kieffer H., Lang H., Matsunaga T., Ono A., Palluconi F., H. Sakuma H., Slater P., Takashima T., Tonooka H., Tsuchida S., Welch R.M., and Zalewski E., 1998: ASTER Preflight and Inflight Calibration and the Validation of Level 2 Products. *IEEE Trans. on Geosc. and R. S.*, **36(4)**:1142-1151.

Vane G., and Goetz, A.F.H., 1988: Terrestrial Imaging Spectroscopy. *Remote Sens. Env.*, **24**:1-29.

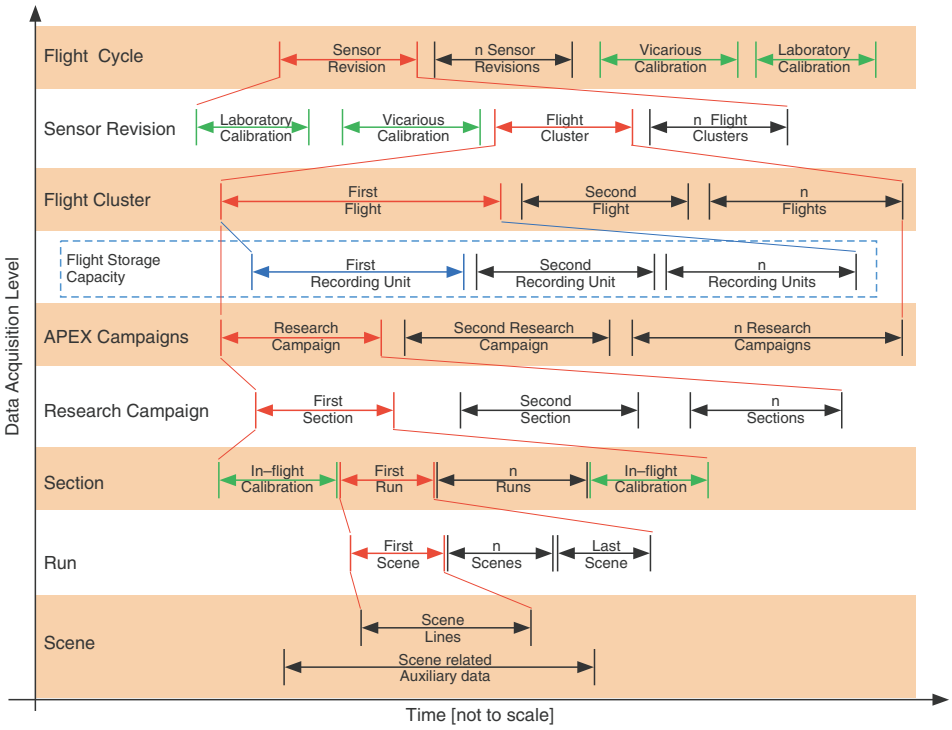

Figure 1: Calibration tasks and data acquisition terminology for APEX flight cycles.

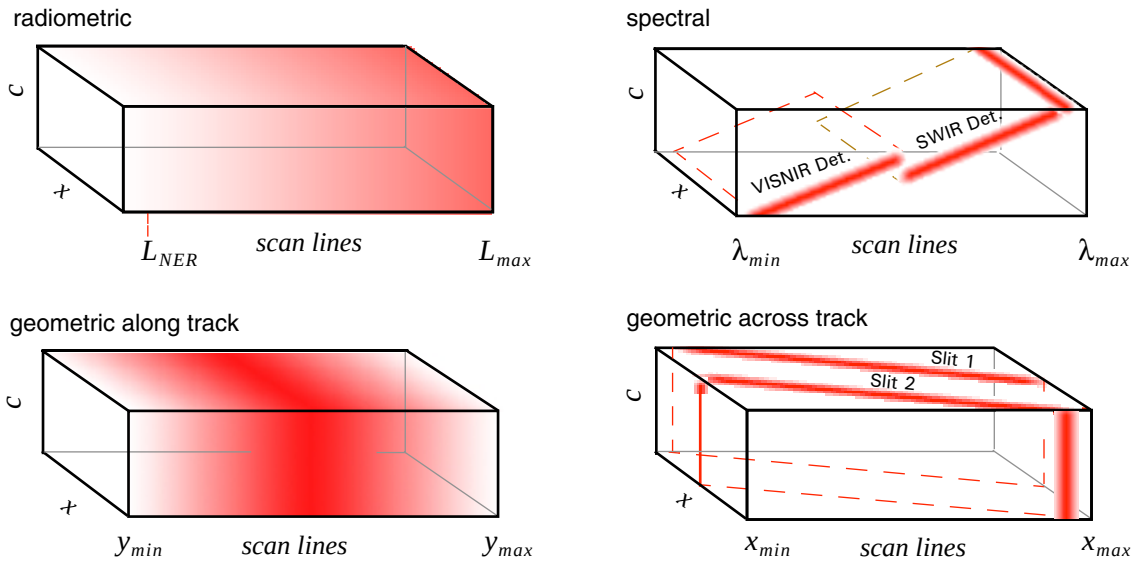

Figure 2: Resulting image cubes from laboratory calibration runs. The grayed areas indicate the measured radiance within the data cubes qualitatively. The wavelength dimension is represented by the spectral bands c which are spectrally overlapping between the two detector arrays.

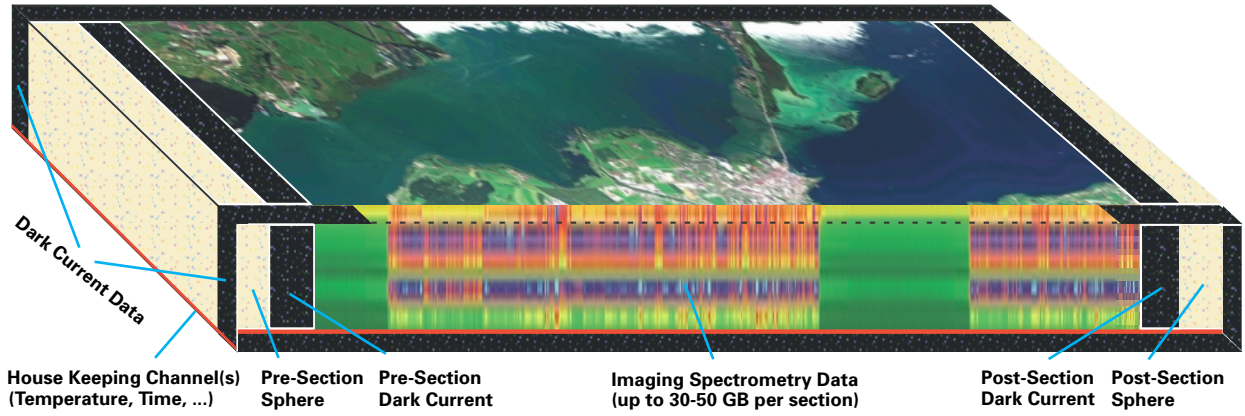

Figure 3: Raw sensor data as acquired by the APEX system, including dark current and measurements of the internal integrating sphere. This cube contains all data acquired for one imaging section (simulation using the HYMAP imaging spectrometer).

(Color Illustration)

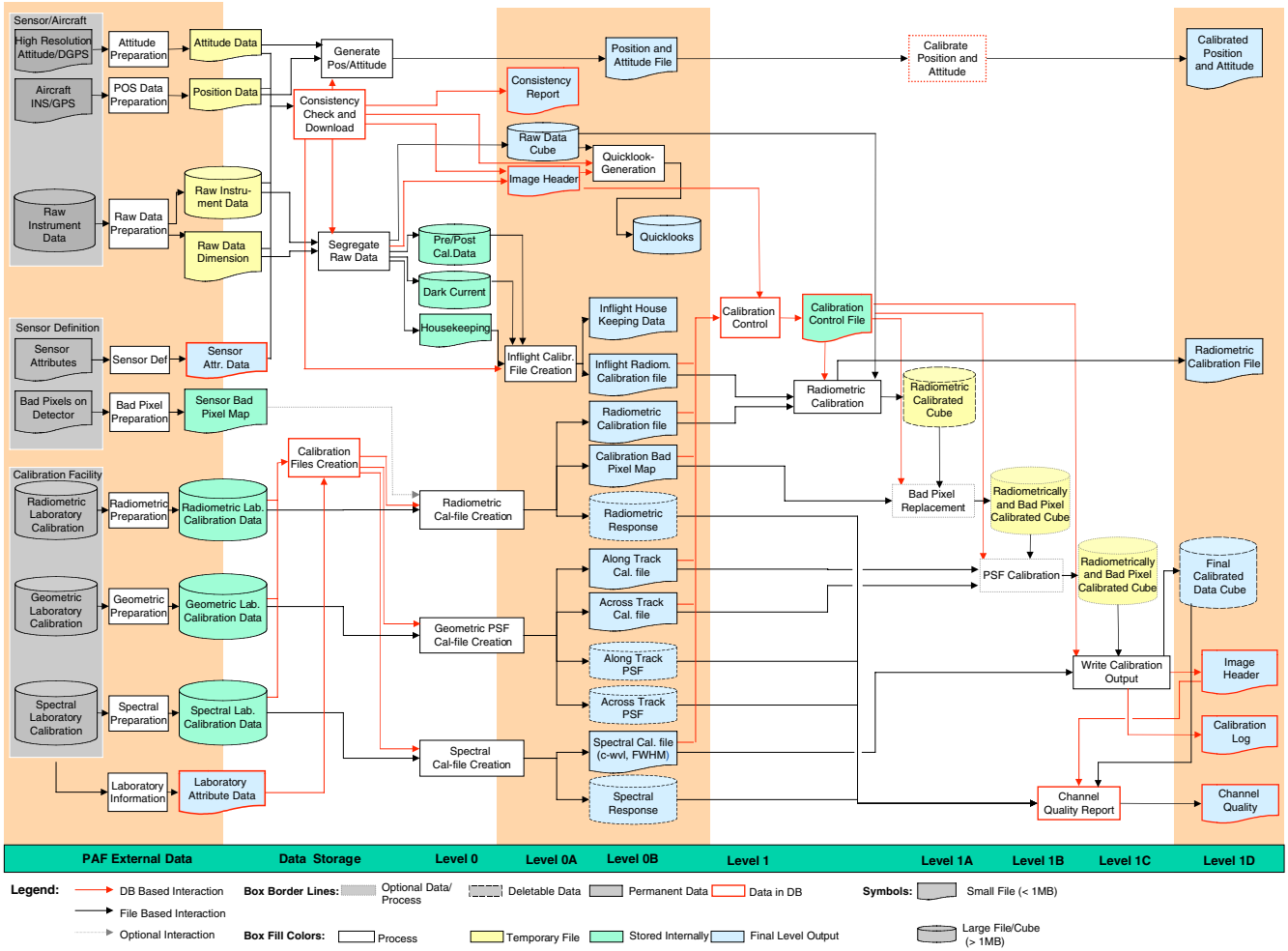

Figure 4: Data preparation and calibration process data flow; red arrows indicate logged interactions of the PAF database system with the processing modules and files, while the effective data flow is depicted with black lines.

(Color Illustration)

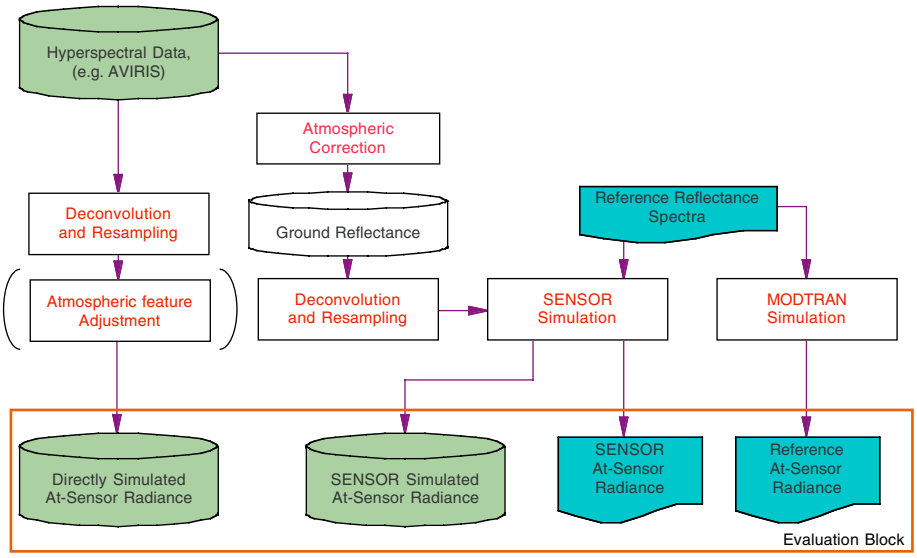

Figure 5: Simulation concept for APEX data based on known hyperspectral data and the SENSOR software tool.

Figure 6: Quality control procedures as foreseen for the APEX calibration. Two major reports are created and validation data are compared to the image data on three levels.